JOURNAL OF MASS SPECTROMETRY
J. Mass Spectrom. 2006; **41**: 1149–1161
Published online 3 August 2006 in Wiley InterScience
(www.interscience.wiley.com) DOI: 10.1002/jms.1067

JMS

Mass spectrometric characterization of covalent modification of human serum albumin by 4-hydroxy-*trans*-2-nonenal

Giancarlo Aldini,* Luca Gamberoni, Marica Orioli, Giangiacomo Beretta, Luca Regazzoni, Roberto Maffei Facino and Marina Carini

Istituto di Chimica Farmaceutica e Tossicologica 'Pietro Pratesi', Faculty of Pharmacy, University of Milan, Viale Abruzzi 42, I-20131 Milan, Italy

Received 18 March 2006; Accepted 22 May 2006

Several pieces of evidence indicate that albumin modified by HNE is a promising biomarker of systemic oxidative stress and that HNE-modified albumin may contribute to the immune reactions triggered by lipid peroxidation-derived antigens. In this study, we found by HPLC analysis that HNE is rapidly quenched by human serum albumin (HSA) because of the covalent adduction to the different accessible nucleophilic residues of the protein, as demonstrated by electrospray ionization mass spectrometry (ESI-MS) direct infusion experiments (one to nine HNE adducts, depending on the molar ratio used, from 1 : 0.25 to 1 : 5 HSA : HNE). An LC-ESI-MS/MS approach was then applied to enzymatically digested HNE-modified albumin, which permitted the identification of 11 different HNE adducts, 8 Michael adducts (MA) and 3 Schiff bases (SB), involving nine nucleophilic sites, namely: His67 (MA), His146 (MA), His242 (MA), His288 (MA), His510 (MA), Lys 195 (SB), Lys 199 (MA, SB), Lys525 (MA, SB) and Cys34 (MA). The most reactive HNE-adduction site was found to be Cys34 (MA) followed by Lys199, which primarily reacts through the formation of a Schiff base, and His146, giving the corresponding HNE Michael adduct. These albumin modifications are suitable tags of HNE-adducted albumin and could be useful biomarkers of oxidative and carbonylation damage in humans. Copyright © 2006 John Wiley & Sons, Ltd.

KEYWORDS: human serum albumin; 4-hydroxy-*trans*-2-nonenal; Michael and Schiff base adduction; ESI-MS direct infusion; LC-ESI-MS/MS analysis

INTRODUCTION

4-Hydroxy-*trans*-2-nonenal (HNE) is the most abundant and toxic α,β-unsaturated aldehyde generated through the β-cleavage of hydroperoxides from ω-6 PUFAs,[1] which plays a key role in a variety of pathophysiological processes, including Alzheimer's and Parkinson's diseases, liver fibrosis, glomerusclerosis, chronic obstructive bronco-pulmonary diseases and atherosclerosis (see reviews[2–5]).

HNE reactivity is due to the conjugation of the double bond with the aldehyde function, which, by tautomeric equilibrium, makes the C-3 carbon a strong electrophilic center, capable of reacting with cellular nucleophiles and, in particular, with the nucleophilic sites of protein (through a Michael addition mechanism), such as the sulfhydryl groups of cysteines, the imidazole moiety of histidines and the ε-amino group of lysine residues.[1] HNE reactivity has been also demonstrated with the ε-amino group of lysine to form a Schiff base, which can eventually lead to the formation of a 2-pentylpirrole through an enammine intermediate.[6] HNE covalently modifies several proteins, as demonstrated by immunological and mass spectrometric methods, among them glucose-6-phosphate dehydrogenase, glyceraldehyde-3-phosphate dehydrogenase, cytochrome-*c* oxidase, hemoproteins, epithelial fatty acid-binding protein, and actin (see review by Carini *et al.*[7]).

In plasma, HNE has been found to modify low-density lipoproteins (LDL). The first report of an interaction of LDL with HNE was by Jurgens *et al.*,[8] and later the HNE binding to the histidine residues of apo B via Michael addition was characterized by Bolgar *et al.*[9] In that report electrospray ionization mass spectrometry (ESI-MS) and ESI tandem MS techniques were used to determine the attachment sites of HNE adducts. LDL probably represent only a minor protein target of HNE, since only 15% of the total plasma HNE–pyrrole immunoreactivity is removed by immunoprecipitation of apo B, thus suggesting that most of the oxidative metabolites generated by lipid oxidation bind to plasma proteins other than LDL.[10] Since albumin is present in high concentration in serum and is characterized by several nucleophilic and accessible residues, it should represent a favorable target protein. The ability of α,β-unsaturated aldehydes to covalently bind albumin has

*Correspondence to: Giancarlo Aldini, Istituto di Chimica Farmaceutica e Tossicologica 'Pietro Pratesi', Faculty of Pharmacy, University of Milan Viale Abruzzi 42, 20131 Milan, Italy.
E-mail: giancarlo.aldini@unimi.it

been previously reported for acrolein and HNE.[11] In particular, by using a 1 : 1 albumin : HNE molar ratio, Bruenner *et al*.[12] found a rapid disappearance of the aldehyde, which after 1 h of incubation was only 3% with respect to the initial amount. Direct evidence of HNE-modified albumin has been reported by Toyokuni *et al*.[13] by using a sandwich enzyme-linked immunosorbent assay, and the basal content in healthy subjects was of 611.4 ± 39.1 pmol ml^{-1}. In that report, it was also found that albumin–HNE adducts are significantly higher in type 2 diabetic patients with respect to control subjects. More recently, Moreau *et al*.[14] profiled HNE-modified proteins in the circulation of both young and old F344 rats by Western blotting analysis and found that serum albumin is the predominant protein adducted by HNE. Albumin–HNE, besides being a promising biomarker of HNE formation in circulation and hence an index of systemic oxidative stress, can also act as an oxidation-specific epitope, a possible immunodominant target of natural antibodies, as recently described for other carbonyl adducted peptides/proteins.[15] As for the immunogenic property of HNE-modified human serum albumin HSA, Traverso *et al*.[16] reported a significant increase of antibody titres against HNE–albumin adduct in diabetic rats, and Mottaran *et al*.[17] found a significant increase of antibodies against HSA-modified by reaction with 4-hydroxynonenal in alcoholic, as compared to nonalcoholic cirrhotic or healthy controls.

Despite the growing interest on albumin–HNE adduction, to our knowledge, no detailed studies on the reaction between HSA and HNE have been reported to date, nor on the chemical characterization of the protein adduct. Hence, the aim of the present investigation was to give evidence that HNE forms covalent addition products with HSA and to identify and characterize the protein modification sites by ESI-MS and LC-ESI-MS/MS experiments.

EXPERIMENTAL

Chemicals

Sequence-grade modified trypsin was obtained from Promega (Milan, Italy) and chymotrypsin from Roche Diagnostics S.p.A. (Monza, Italy). Iodoacetamide, (±)-*threo*-1,4-dimercapto-2,3-butanediol (DTT) and delipidized HSA (~99% agarose gel electrophoresis) were from Sigma–Aldrich (Milan, Italy). 4-Hydroxy-non-2-enal diethylacetal (HNE-DEA) was prepared as reported by Rees *et al*.[18] and HNE by HNE–DEA hydrolysis with 1 mM HCl (1 h at room temperature) and titrated by UV spectroscopy (λ_{max} 224 nm; ε 13 750 l mol^{-1} cm^{-1}). LC-grade and analytical-grade organic solvents were purchased from Merck (Bracco, Milan, Italy). LC-grade water was prepared with a Milli-Q water purification system (Millipore, Bedford, MA, USA). All other reagents were of analytical grade.

HNE incubation with HSA and HPLC analysis

HNE (10 μM) was incubated with commercial HSA (600 μM) in 10 mM phosphate buffer (pH 7.4) at 37 °C. Samples corresponding to different incubation time (200 μl) were deproteinized with 0.7 mM perchloric acid (200 μl), centrifuged at 18 000*g* for 10 min and the supernatants analyzed by HPLC to measure HNE consumption, as previously described.[19]

In vitro modification of isolated HSA by HNE

Blood collected by venopuncture from two male healthy volunteers was allowed to clot at room temperature for no longer than 30 min and centrifuged for 10 min at 1500*g*. Serum aliquots were then stored in liquid nitrogen until further use. Serum albumin was isolated using the Montage Albumin Deplete Kit (Millipore, Milan, Italy) and eluted with 1 M NaCl. HSA concentration was measured by its absorbance at 279 nm (E1% 1 cm = 5.31). Samples were then desalted on Microcon centrifugal filter devices (Millipore, Milan, Italy) by rinsing with distilled water, and diluted with 20 mM phosphate buffer saline (PBS, pH 7.4) to a final concentration of 20 μM. HNE was then added at the following HSA : HNE final molar ratios: 1 : 0.25; 1 : 0.5; 1 : 1 and 1 : 5. After 120 min incubation at 37 °C, samples were incubated at room temperature for additional 60 min with $NaBH_4$ (final concentration 5 mM), and then desalted by Microcon filter devices as described above, liophylized and stored in liquid nitrogen until the analysis.

Mass spectrometry

Direct infusion electrospray mass spectral analysis (ESI-MS): triple quadrupole (TQ) mass spectrometer

To detect changes in protein mass and to determine the stoichiometry of reaction, undigested native and HNE-treated HSA were analyzed by direct infusion on a triple-quadrupole (TQ) mass spectrometer (Finnigan TSQ Quantum Ultra, ThermoQuest, Milan, Italy) equipped with an Electrospray Finnigan Ion Max source. The lyophilized protein (250 μg) was dissolved in 200 μl of water, mixed with 200 μl of CH_3CN–H_2O–HCOOH (30 : 70 : 0.4, v/v/v) and infused into the mass spectrometer at a flow rate of 5 μl min^{-1}. Each sample was analyzed using two different mass ranges: m/z 900–1500 (Q = m/z 1) and m/z 1410–1500 (Q = m/z 0.5), under the following instrumental conditions: positive-ion mode; capillary temperature 270 °C; spray voltage applied to the needle 3 kV; capillary voltage 46 V; nebulizer gas (nitrogen) flow rate set at 0.5 l min^{-1}; acquisition time 10 min.

Liquid chromatography electrospray ionization mass spectrometry/mass spectrometry analysis (LC-ESI-MS/MS): ion trap mass spectrometer

Tryptic peptide maps were generated by LC-ESI-MS/MS analysis in data-dependent scan mode and dynamic exclusion in positive-ion mode. For sample preparation, the lyophilized target protein (420 μg) was dissolved in 100 μl 50 mM Tris-HCl (pH 7.8) and digested according to the manufacturer's procedure. Aliquots of 10 μl of the digested samples were injected into a quaternary pump HPLC system (Surveyor LC system, ThermoQuest, Milan, Italy). Separations were done by reversed-phase elution with an Agilent Zorbax SB-C18 column (4 mm i.d., particle size 3.5 μm) (CPS Analitica, Milan, Italy) protected by an Agilent Zorbax R-P guard column, thermostatted at 25 °C. An 80-min linear gradient from 100% A (0.1% HCOOH in water) to 60% B (CH_3CN : H_2O : HCOOH; 90 : 10 : 0.1, v/v/v) followed by a 20 min equilibration period was used to elute the digested peptides; the mobile phase was delivered at a flow rate of 0.2 ml min^{-1}. ESI-MS analyses were carried out using a

DOI: 10.1002/jms

Finnigan LCQ Advantage Ion trap mass spectrometer (ThermoQuest, Milan, Italy); the ESI source was set in positive-ion mode, under the following conditions: capillary temperature 250 °C; spray voltage 4.5 kV; source current 10 μA; capillary voltage 10.0 V. The flow rate of the nebulizer gas (nitrogen) was 5 l min^{-1}. MS/MS analyses were carried out in data-dependent scan mode, and enabling the dynamic exclusion under the following conditions: repeat count 1; repeat duration 0.5 min; exclusion duration 2 min.

Peptide adducts identification

Peptide ion responses were determined by measuring the peak areas in the selected ion chromatograms (SICs) reconstituted by using the $[M + H]^+$ as filter ions. When the $[M + H]^+$ ion of the target peptide exceeded 2000 Da, or when it was characterized by a low ionic response, the next well-detectable charge state ion was selected. The peptide responses were normalized in respect to peptide T53 (LVAASQAALGL), chosen as reference peptide because it does not contain nucleophilic residues. Loss of specific peptides in HNE-treated HSA with respect to native HSA was determined by calculating the relative peptide consumption using the following equation: peptide consumption (%) $= 100 - [(A_{HNE})/(A_{NATIVE}) \times 100]$ where A_{HNE} and A_{NATIVE} are the normalized peptide ion response of the target peptide from HSA incubated in presence of and in the absence of HNE, respectively. For each peptide undergoing a consumption over a threshold of 10%, the $[M + H]^+$ and the +2, +3, +4 and +5 multicharged state ions were predicted for the following potential $NaBH_4$-reduced HNE adducts: (1) HNE Schiff base adduct (SB-HNE; +140 Da) for Lys containing peptides; (2) HNE-Michael adduct (MA-HNE; +158 Da) for His, Lys and Cys containing peptides; (3) the combination of the above-considered adducts for peptides containing more than one nucleophilic residue. Moreover, since the trypsin is unable to cleave the protein at adducted Lys residues, predicted ions relative to missed cleavage adducted peptides were also considered. The SIC traces were then reconstituted using for filter ions the predicted ion values and the HNE adducts were identified as detailed in the results session.

Bioinformatics

Direct infusion ESI-MS spectra were deconvoluted using the software package Bioworks 3.1 (ThermoQuest, Milan, Italy) and MagTran 1.02.[20] Peptide sequences were identified using the software turboSEQUEST (Bioworks 3.1, ThermoQuest, Milan, Italy), and using a database containing only the protein of interest and assuming trypsin digestion. *In silico* tryptic digest of HSA was also used as aid for peptide identification. The protein sequence of human serum albumin was obtained from the Swiss-Prot database (primary accession number P02768). PEPTIDEMASS was used to calculate theoretical digested masses on the basis of tryptic digest and setting all Cys as carbamidomethylcysteine.[21] Predicted y and b series ions were determined by using the Peptide Sequence Fragmentation Modeling, Molecular Weight Calculator software program (ver. 6.37), http://come.to/alchemistmatt. Xcalibur software provided instrument control and data analysis for the Thermo Electron mass spectrometers.

RESULTS

HNE quenching by HSA

The ability of HNE to react with HSA was first assayed by monitoring the HNE consumption in a reaction mixture containing 600 μM HSA (the mean plasma concentration) and 10 μM HNE, a concentration found in plasma, various organs and cell types under oxidative stress conditions.[22,23] As shown in Fig. 1, HSA induced a rapid disappearance of the aldehyde, characterized by an exponential decay (goodness to fit: $R^2 = 0.994$) and reaching 50% of the initial amount within 60 s, thereby indicating the high reactivity of HNE towards HSA.

Covalent binding of HNE to HSA: direct infusion ESI-MS analysis

In preliminary experiments, commercial HSA was used to study the covalent adduction of HNE by mass spectrometry. Although under these conditions the formation of HNE adducts was clearly evident, the spectra were poorly resolved and the ion peaks significantly broadened, thereby greatly affecting the quality of the MS spectra (data not shown). We then decided to use HSA isolated from human serum by affinity chromatography. Figure 2 (panel A), shows the positive-ion ESI mass spectrum of serum HSA (scan-range m/z 900–1500), showing multiply charged peaks ranging from m/z 1073 to m/z 1478 and corresponding to the addition of 62 to 45 protons. To further enhance the MS resolution, a reduced scan range m/z 1410–1500 was used in order to acquire the MS spectrum for 10 min at m/z 0.5 resolution. Figure 2 (panel B) shows the ESI-MS spectrum in positive-ion mode of native HSA, characterized by three abundant ions at m/z 1414.8, 1445.5 and 1477.2, and attributed to the +47, +46 and +45 multicharged ions of native HSA

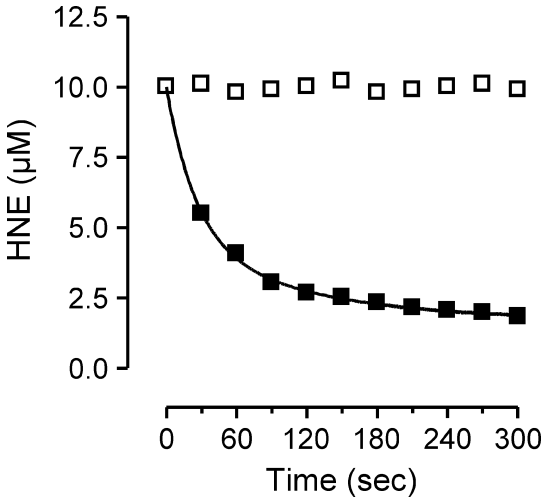

Figure 1. Kinetics of HNE reaction with HSA. Time-dependent consumption of 10 μM HNE in the absence (□) and in presence (■) of 600 μM HSA in 10 mM phosphate buffer (pH 7.4, 37 °C). At each time point, the HNE content was determined by HPLC analysis as described in the 'Experimental' section.

DOI: 10.1002/jms

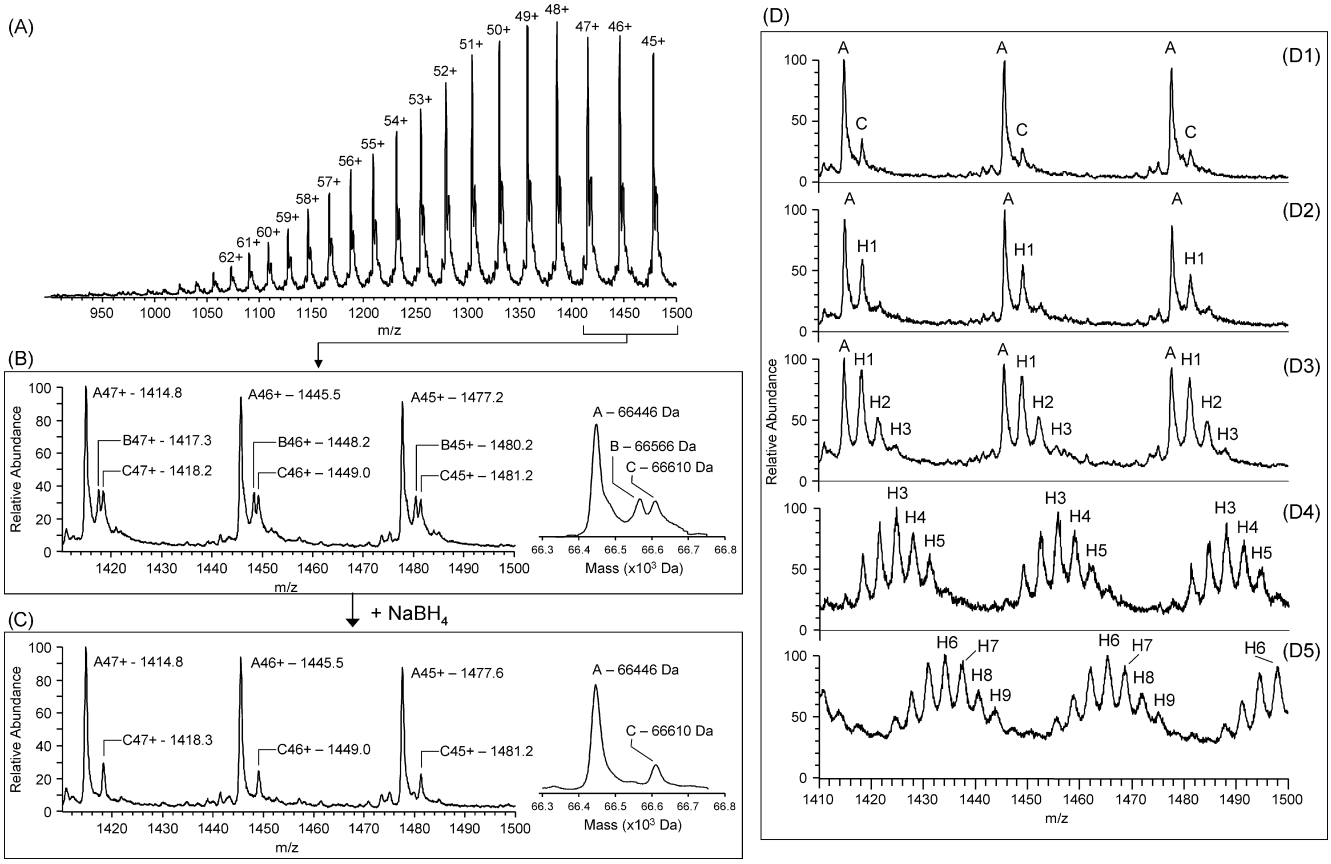

Figure 2. Direct infusion ESI-MS analysis of native HSA and stoichiometry of HNE-adduction. ESI-MS spectrum of isolated serum HSA using mass ranges m/z 900–1500 (panel A) and m/z 1410–1500 (panel B). Panel C shows the mass spectrum of HSA after $NaBH_4$ reduction for 60 min. On the right side of panels B and C are depicted the deconvoluted spectra. Panel D: stoichiometry of HNE adduction to HSA as determined by direct infusion ESI-MS analysis. HSA was incubated for 2 h at 37 °C in the absence (D1) and presence of HNE at the following HSA : HNE molar ratios: 1 : 0.25 (D2); 1 : 0.5 (D3); 1 : 1 (D4) and 1 : 5 (D5).

(compound A). The MS spectrum is also characterized by other two ions series at m/z 1417.3, 1448.2, 1480.2 (compound B) and at m/z 1418.2, 1449.0, 1481.2 (compound C), reaching a relative abundance of 30–35% with respect to native HSA. The deconvoluted spectrum shows a molecular weight of 66 446 Da for compound A, which is in good agreement with the theoretical value of 66 429 ($\Delta m = +17$ Da) based on the amino acid sequence (SwissProt entry number P02768), thereby exhibiting good precision. The MW of compounds B and C are 66 566 Da and 66 610 Da, respectively, corresponding to a +120 and +164 Da mass increase in respect to native HSA and attributed to the addition of a cysteine residue through a disulfide bond (theoretical increment +119 Da) and to the addition of glucose to a protein amino group (+162), as recently reported by others.[24,25] When native HSA was treated with $NaBH_4$, a reducing agent used to stabilize carbonyl-derived Michael and Schiff base adducts with protein nucleophilic sites,[26] compound B completely disappeared owing to the reduction of the disulfide bond, while the glycated derivative remained unchanged, as expected (Fig. 2, panel C). Since the MS spectra of native HSA were satisfactory enough in terms of signal-to-noise ratio and resolution, these experimental conditions were used to study the HNE adduction to HSA by direct infusion ESI-MS analysis. When HSA was incubated in the presence of HNE at a molar ratio 1 : 0.25 for 2 h at 37 °C, a well-detectable HNE adduct (H1), shifted by +160 Da with respect to native HSA, was observed and attributed to a HNE Michael adduct (theoretical mass increment +158) (Fig. 2, panel D2). By increasing the HNE concentration (1 : 0.5 molar ratio, panel D3), the relative abundance of H1 increased to reach that of native HSA, and a second adduct (H2), characterized by a mass increase of +142 Da with respect to H1, became well detectable, which could be tentatively assigned the structure of a HNE Schiff base adduct (theoretical mass increment: +140). In addition, a third Michael HNE-adduct was also evident, although present in smaller amount (H3). At a 1 : 1 molar ratio (panel D4), the multicharged ion peaks relative to native HSA almost completely disappeared and concomitantly the formation of five ions series was observed (H1 → H5), which increased up to nine HNE-adducts in the presence of an excess of the aldehyde (1 : 5 molar ratio, panel D5).

Identification of HNE-adducted peptides by LC-ESI-MS/MS

To characterize the structural modification of HSA induced by HNE, native and HNE-treated HSA were reduced by $NaBH_4$, an established procedure for adduct stabilization, digested with proteolytic enzymes and analyzed by LC-ESI-MS/MS. When trypsin was used as the proteolytic

DOI: 10.1002/jms

enzyme, peptide mass mapping provided identification of the peptides, accounting for approximately 78% of the protein sequence (Table 1).

Quenching-peptide method

Owing to the complexity of the LC-ESI-MS/MS chromatogram (data not shown), HNE-adducted peptides were first identified as those peptides undergoing significant consumption with respect to the peptides from native HSA. As shown in Fig. 3, eight peptides underwent a consumption over 10% (chosen as threshold level) by adding HNE at a final molar ratio HSA : HNE 1 : 5, namely, T3, T6, T14, T18, T25, T29, T47 and T49. As a second step, on the basis of the sequence of the quenched peptides, the MW and the corresponding single and multicharged state ions for each potential HNE adducts were predicted. In particular, His-containing peptides were predicted as HNE Michael adduct (+158), and Lys-containing peptides as Michael (+158) and Schiff base (+140) adducts. When a target peptide contained more than one His or Lys residue or a mixture of them, the different combinations were taken into account. Moreover, by considering that trypsin is unable to cleave the protein at adducted Lys residues, merged peptides due to missed cleavages were considered, together with the HNE-Lys Michael or Schiff base adduction. The SIC traces were then reconstituted using for filter ions the predicted ion values. HNE-adducts were identified when both the following criteria were satisfied: (1) the SIC traces reconstituted for the predicted HNE-adducts showed a well detectable peak in the HNE-treated sample, absent in native HSA; (2) the relative area of the HNE-adduct (calculated in respect to the reference peptide T53), increased with respect to the molar ratio. By using this approach, eleven HNE-modified peptides were identified (Table 2) and for each of them a detailed description is reported below.

Lys199

Peptide T18 contains two nucleophilic sites, Cys200 and Lys205. Both the residues are excluded as adduction sites of HNE: Cys200 is found in native protein as disulfide and Lys205 adduction would provide a missed cleavage, giving a merged product with peptide T19. Since peptide T19 was not found significantly reduced, we can exclude Lys205 as an HNE adduction site. A possible explanation for the reduction of peptide T18 would be to consider Lys199 as reaction site: in such a case, the tryptic dipeptide Leu198-Lys199 (not identified in the mapping peptide) would merge with peptide T18, giving the adducted and merged peptide LKCASLQK. On the basis of this hypothesis, we predicted two multicharged ion series, one containing HNE as MA-HNE (predicted MW = 1104.7 Da) and the other as SB-HNE (predicted MW = 1086.6 Da). The ion traces relative to native and HNE-adducted peptides are shown in Fig. 4, and clearly indicate that HNE covalently binds to Lys199 through both a Michael (peptide H-T3, Table 2) and a Schiff base (peptide H-T4) mechanism. The MW of the two adducts, as determined by deconvoluting the multicharged ions of MS spectra relative to the reconstituted peaks (Fig. 4, panel C and F) are in agreement with the theoretical values. Sequencing

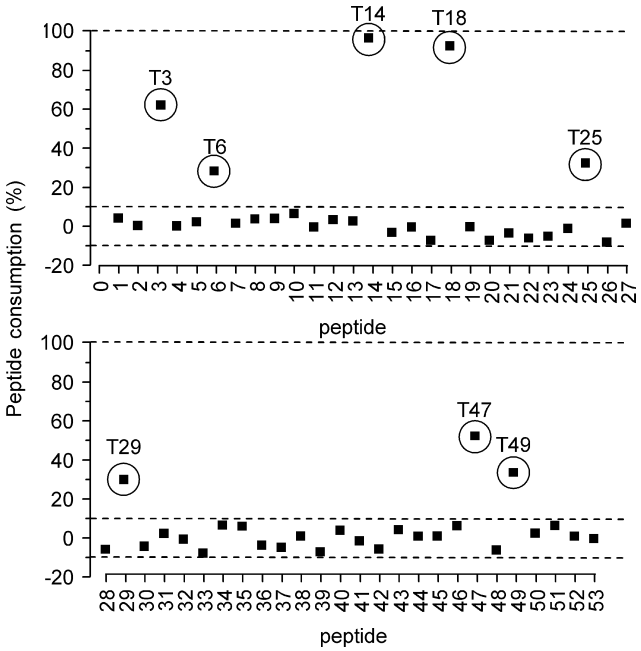

Figure 3. HSA-peptide consumption induced by HNE exposure. Relative HSA-peptides consumption induced by HNE incubation (HSA : HNE 1 : 5 molar ratio). Peptides T3, T6, T14, T18, T25, T29, T47 and T49 are characterized by consumption greater than 10% set as threshold level. Peptides were obtained by HSA trypsin digestion and the ion response and relative consumption calculated as described in the 'Experimental' section.

by MS/MS was used to confirm the identities of the adducted peptides and to identify the site of adduction. The MS^2 spectra of MA and BS adducts of the adducted peptide are shown in Fig. 4. Assignment of Lys199 as the adduction site of HNE-MA adduct was provided by the MS^2 spectrum of the $[M + H]^+$ m/z 1105.5, which showed the y_6 ion at m/z 706.3, the adducted $y_7{}^{*2+}$ ion at m/z 496.5 and b_3^* at m/z 560.3 (Fig. 4 panel G). Identification of the HNE Schiff adduct on Lys199 was obtained by the MS^2 analysis of the parent-ion at m/z 544.7, showing the y_6 ion at m/z 706.3, $y_7^* - H_2O$ at m/z 956.4 and b_2^* ion shifted by +158 Da at m/z 382.6 (Fig. 4 panel H).

Lys525

Since Lys525 has been reported to be an important adduct-binding site of HSA,[28] consumption of peptide T49 (QTALVELVK) was first explained by considering the formation of the merged peptide KQTALVELVK as a consequence of the covalent adduction to Lys525, and the multicharged ions relative to the corresponding MA and SB HNE adducts were predicted. The reconstituted ion traces evidence the formation of both the adducts (Fig. 5). The MS^2 spectrum of the $[M + 2H]^{2+}$ parent ion at m/z 644.0 relative to the MA adduct shows an unmodified partial y-ion series (up to y_8) and $b_2{}^*$ ion shifted by 158 Da, identifying Lys525 as the adduction site (Fig. 5, panel G). Lys525 was also found as the adduction site of the SB adduct, as evidenced by the MS^2 spectrum of the $[M + 2H]^{2+}$ parent ion at m/z 635.3, characterized by the

DOI: 10.1002/jms

Table 1. Peptides identified by LC-ESI-MS/MS from native HSA digested with trypsin

Peak no.	Sequence position	Sequence	Mass (calc.)[a]	Mass (obs.)	R.T. (min)
T1	5–10	SEVAHR	697.4	697.8	9.15
T2	13–20	DLGEENFK	950.4	950.8	36.07
T3	21–41	ALVLIAFAQYLQQC°PFEDHVK	2489.3	2489.8	76.62
T4	42–51	LVNEVTEFAK	1148.6	1149.1	44.35
T5	52–64	TC°VADESAENC°DK	1497.6	1498.5	26.72
T6	65–73	SLHTLFGDK	1016.5	1017.5	41.91
T7	74–81	LC°TVATLR	932.5	932.5	37.66
T8	82–93	ETYGEMADCCAK	1433.5	1433.4	33.55
T9	94–98	QEPER	657.3	657.3	13.05
T10	99–106	NEC°FLQHK	1074.5	1075.5	31.19
T11	107–114	DDNPNLPR	939.4	940.0	30.40
T12	115–136	LVRPEVDVMC°TAFHDNEETFLK	2649.2	2650.8	57.52
T13	138–144	YLYEIAR	926.5	926.5	42.80
T14	146–159	HPYFYAPELLFFAK	1741.9	1741.9	70.19
T15	163–174	AAFTEC°C°QAADK	1370.6	1371.5	31.29
T16	175–181	AAC°LLPK	771.4	771.4	36.57
T17	182–186	LDELR	644.3	644.5	29.09
T18	200–205	C°ASLQK	705.3	705.4	18.65
T19	206–209	FGER	507.2	507.5	19.73
T20	210–212	AFK	364.2	364.2	9.66
T21	213–218	AWAVAR	672.4	672.8	33.69
T22	219–222	LSQR	502.3	502.5	7.91
T23	226–233	AEFAEVSK	879.4	879.4	31.98
T24	234–240	LVTDLTK	788.5	788.5	34.80
T25	241–257	VHTEC°C°HGDLLEC°ADDR	2085.8	2087.1	35.56
T26	258–262	ADLAK	516.3	516.2	14.31
T27	263–274	YIC°ENQDSISSK	1442.6	1443.4	32.03
T28	277–286	EC°C°EKPLLEK	1304.6	1305.4	31.19
T29	287–313	SHC°IAEVENDEMPADLPSLAADFVESK	2973.3	2974.0	66.65
T30	314–317	DVC°K	520.2	520.1	6.84
T31	318–323	NYAEAK	694.3	673.6	17.85
T32	324–336	DVFLGMFLYEYAR	1622.8	1623.9	76.14
T33	338–348	HPDYSVVLLLR	1310.7	1311.4	56.48
T34	352–359	TYETTLEK	983.5	983.4	31.67
T35	360–372	C°C°AAADPHECYAK	1551.6	1552.3	27.64
T36	373–389	VFDEFKPLVEEPQNLIK	2044.1	2043.9	60.59
T37	390–402	QNC°ELFEQLGEYK	1656.7	1657.0	54.04
T38	403–410	FQNALLVR	959.6	959.6	44.83
T39	411–413	YTK	410.2	410.2	6.14
T40	415–428	VPQVSTPTLVEVSR	1510.8	1510.7	48.00
T41	429–432	NLGK	430.2	430.2	8.79
T42	440–444	HPEAK	580.3	580.2	5.99
T43	446–466	MPC°AEDYLSVVLNQLC°VLHEK	2517.2	2517.2	76.39
T44	467–472	TPVSDR	673.3	673.6	18.05
T45	476–484	C°C°TESLVNR	1137.5	1137.8	31.56
T46	485–500	RPC°FSALEVDETYVPK	1910.0	1910.4	51.04
T47	501–519	EFNAETFTFHADIC°TLSEK	2259.0	2260.0	57.75
T48	522–524	QIK	387.2	387.2	6.12
T49	526–534	QTALVELVK	999.6	999.6	47.72
T50	542–545	EQLK	516.3	516.0	11.56
T51	546–557	AVMDDFAAFVEK	1341.6	1341.8	60.32
T52	565–573	ETC°FAEEGK	1069.4	1070.2	29.40
T53	575–585	LVAASQAALGL	1012.6	1012.0	52.37

[a] Isotopic MW; ° = carboimidomethyl-cysteine.

DOI: 10.1002/jms

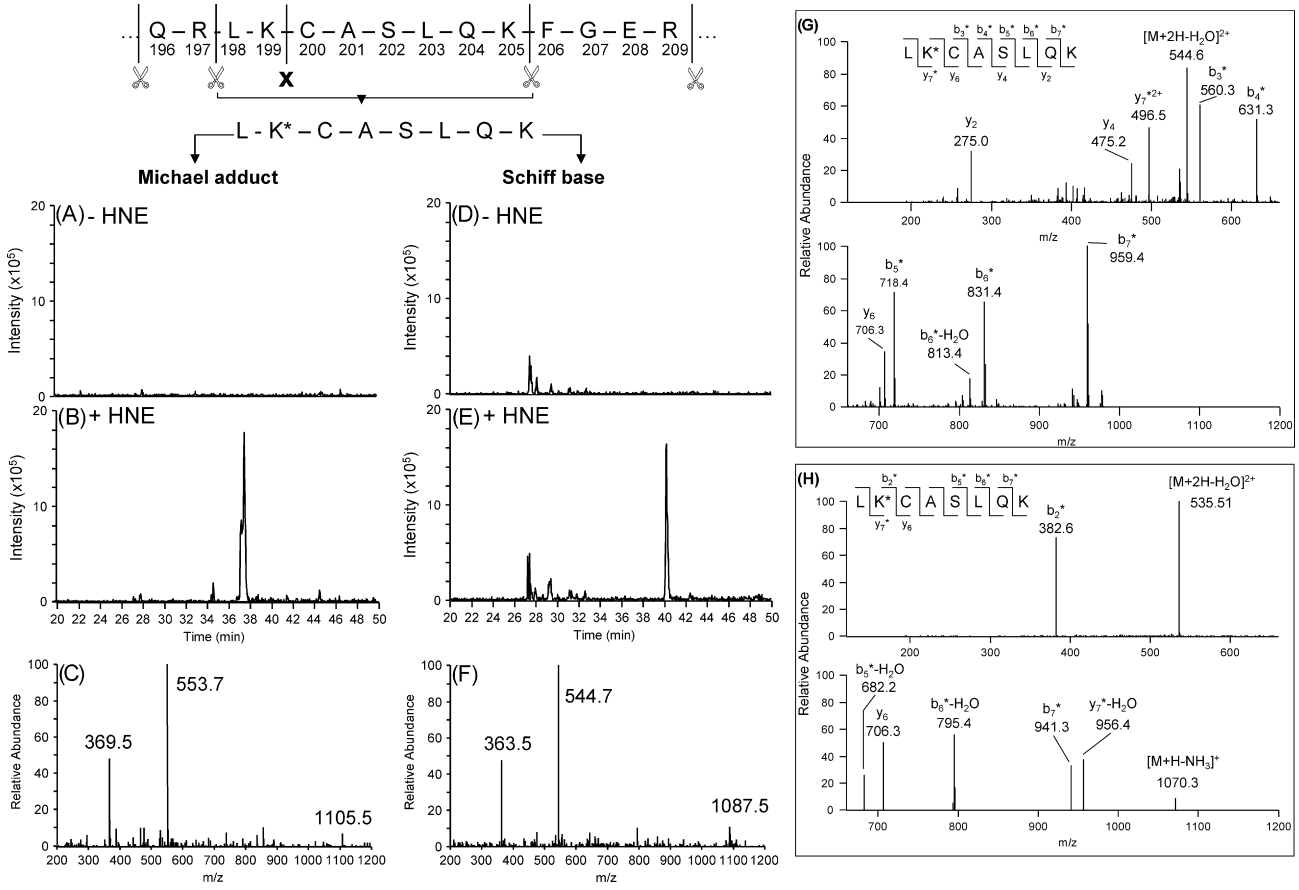

Figure 4. Identification of H-T3 and H-T4 HNE-adducted peptides and Lys199 as adduction site by LC-ESI-MS/MS analysis. Panels A, B: SICs relative to the ions $[M + H]^+$ m/z 1105.7 and $[M + 2H]^{2+}$ m/z 553.3 relative to the predicted MA-HNE adduct of the merged peptide LKCASLQK. The samples are relative to HSA incubated for 2 h at 37 °C in absence (panel A) and presence of HNE (panel B) (molar ratio HSA : HNE of 1 : 5) and then digested with trypsin. Panel C shows the MS spectrum relative to the peak at R.T. 37.3 min (observed mass by deconvolution analysis: 1104.7 Da; calculated mass: 1104.7 Da). Panels D, E: SICs relative to ions $[M + H]^+$ m/z 1087.6 and $[M + 2H]^{2+}$ m/z 544.3 of the predicted SB-HNE adduct of LKCASLQK peptide. The samples are relative to tryptic digested HSA incubated in absence (panel D) and presence (panel E) of HNE, respectively. MS spectrum relative to the peak with an R.T. of 40.0 is depicted in panel F (observed mass by deconvolution analysis: 1086.1 Da; calculated mass: 1086.6 Da). Panels G, H: LC-ESI-MS/MS spectra of the adducted peptides H-T3 (parent-ion m/z 1105.5, panel G) and H-T4 (parent ion m/z 544.7, panel H). Lys199 was identified as the adduction site. Modified fragment ions are labeled with an asterisk and are according to the nomenclature of peptide fragmentation.[27]

partial y-series (y_2, y_3, y_4, y_7, y_8 and y_9) and by the presence of the b_2^* ion at m/z 397.2 (Fig. 5, panel H).

His 67

Peptide T6 was significantly reduced, although to a lesser extent with respect to other nucleophilic peptides (Fig. 3). The reconstituted SIC trace relative to the corresponding MA well evidences a peak at R.T. 57.2 min in HNE-treated albumin, which was absent in native HSA (data not shown). The HNE-adducted peptide was easily identified by product ion analysis of the $[M + 2H]^{2+}$ parent ion at m/z 588.3. His67 was identified as the adduction site by considering the unchanged y_6 at m/z 680.2 and y_7^{*2+} ion at m/z 488.4, as well as the b_3^* ion at m/z 496.2 (data not shown).

His146

Peptide T14 contains two nucleophilic sites: Lys159 and His146, the latter recognized as an important adduct-binding site of HSA. However, in the trypsin-digested mixture, the reconstituted ion traces relative to the different combination of adducts did not show the formation of any predicted adducts. The adducted peptide was identified in the trypsin/chymotrypsin reaction mixture as the MA of peptide HPY (H-TC2, Table 2) (Fig. 6). Definitive assignment was obtained by MS^2 analysis of the $[M + H]^+$ at m/z 574.3, showing the His–HNE immonium ion at m/z 268.2, and the adducted b-ion series b_1^* and b_2^* at m/z 296.0 and 393.2, respectively (Fig. 6, panel G).

His242

Peptide T25 contains two His residues as potential HNE-MA adduct sites, namely, His242 and His247. Hence two adducted peptides were predicted, one containing one HNE-MA adduct (+158, predicted MW = 2243.8 Da), and the second containing two HNE derivatives (+316, MW = 2401.8 Da). By reconstituting the SIC traces of the predicted ions, only a mono HNE adduct was found in the tryptic digest (H-T5, Table 2)(Fig. 6, right panel). The

DOI: 10.1002/jms

Table 2. Identified HNE-adducted peptides after enzymatic digestion (trypsin and trypsin + chymotrypsin) of HSA incubated with HNE (HSA : HNE 1 : 5 molar ratio) for 120 min at 37 °C. * = HNE-adducted site; ° = carboimidomethyl-cysteine

	Adducted peptide sequence	Adducted AA	Type of adduct	Predicted multicharged ions				RT (min)
				+1	+2	+3	+4	
H-TC1	LQQC*PF	Cys34	MA	893.5	447.2	–	–	64.8–65.7
H-T1	SLH*TLFGDK	His67	MA	1175.7	588.3	392.6	–	57.2
H-TC2	H*PY	His146	MA	574.3	–	–	–	40.5
H-T2	ASSAK*QR	Lys195	SB	887.5	444.3	296.5	–	27.8
H-T3	LK*CASLQK	Lys199	MA	1105.7	553.3	–	–	37.3
H-T4	LK*CASLQK	Lys199	SB	1087.6	544.3	–	–	40.0
H-T5	VH*TEC°C°HG DLLEC°ADDR	His242	MA	–	1123.0	749.0	–	42.9
H-T6	SH*C°IAEVE NDEMPADL PSLAADFVESK	His288	MA	–	1566.7	1044.8	783.9	70.3
H-T7	EFNAETFTFH* ADIC°TLSEK	His510	MA	–	1209.6	806.7	–	65.5
H-T8	K*QTALVELVK	Lys525	MA	1286.8	643.9	–	–	53.5
H-T9	K*QTALVELVK	Lys525	SB	1268.8	634.9	–	–	56.1

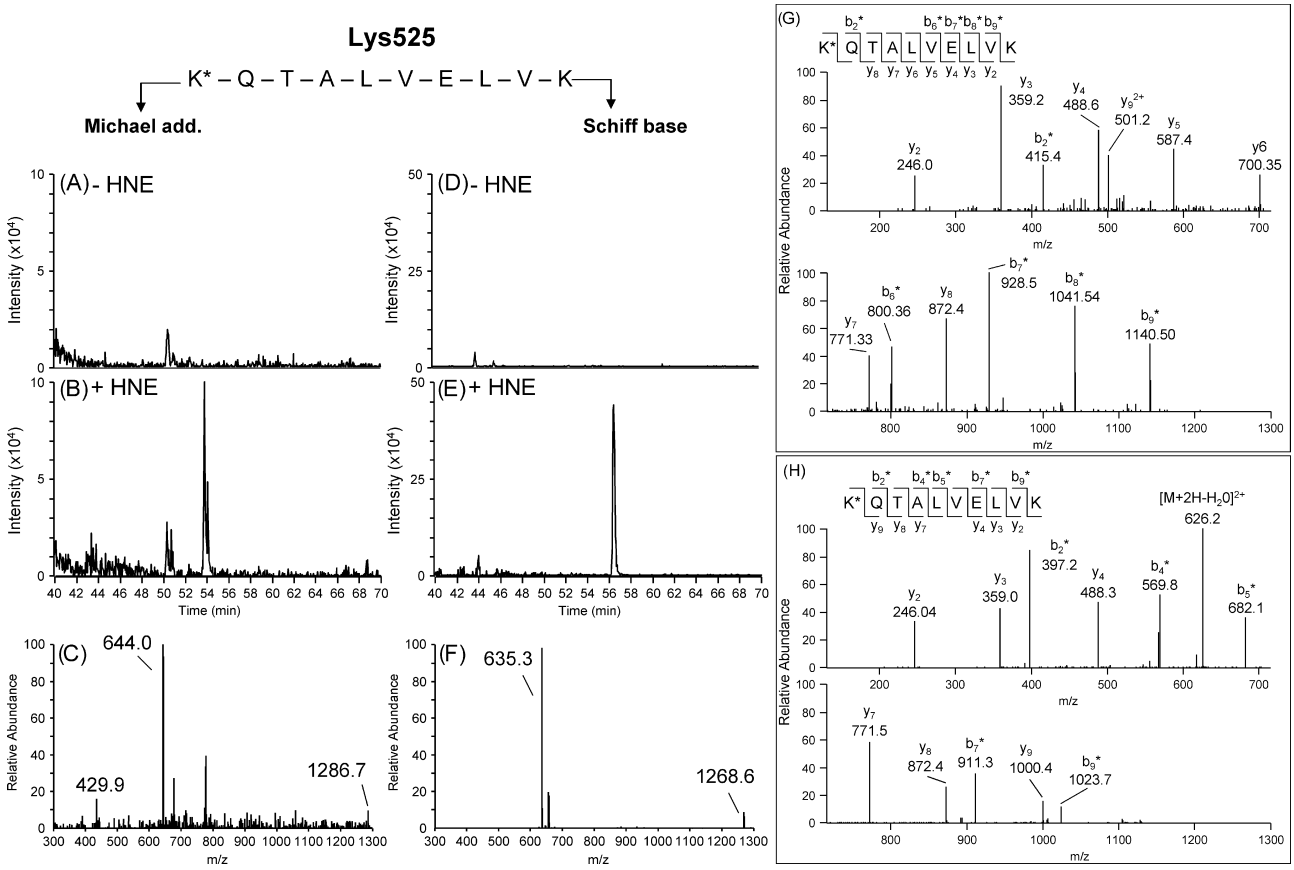

Figure 5. Identification of H-T8 and H-T9 HNE-adducted peptides and Lys525 as adduction site by LC-ESI-MS/MS analysis. Panels A, B, C: SICs relative to the ions $[M + H]^+$ m/z 1286.8 and $[M + 2H]^{2+}$ at m/z 643.9 relative to the predicted MA-HNE adduct of the merged peptide KQTALVELVK. HSA was incubated for 2 h at 37 °C in the absence (panel A) and presence of HNE (panel B), at a molar ratio HSA : HNE of 1 : 5. Panel C shows the MS spectrum relative to the peak at RT 53.5 min (observed mass by deconvolution analysis: 1285.3 Da; calculated mass: 1285.8 Da). Panels D, E, F: Panels D and E show the SICs relative to the predicted SB-HNE adduct ions at m/z 1268.8 $[M + H]^+$ and m/z 634.9 $[M + 2H]^{2+}$ of the merged peptide KQTALVELVK. HSA was incubated for 2 h at 37 °C in absence (panel D) and presence of HNE (panel E), at a molar ratio HSA : HNE of 1 : 5. MS spectrum relative to the peak with an R.T. of 56.1 is depicted in panel F (observed mass by deconvolution analysis: 1267.7 Da; calculated mass: 1267.8 Da). Panels G, H: LC-ESI-MS/MS spectra of HNE-adducted peptides H-T8 (parent-ion m/z 644.0, panel G) and H-T9 (parent-ion m/z 635.3, panel H). Lys525 is identified as adduction site. The symbol * denotes the shifted peptide in respect to native HSA.

DOI: 10.1002/jms

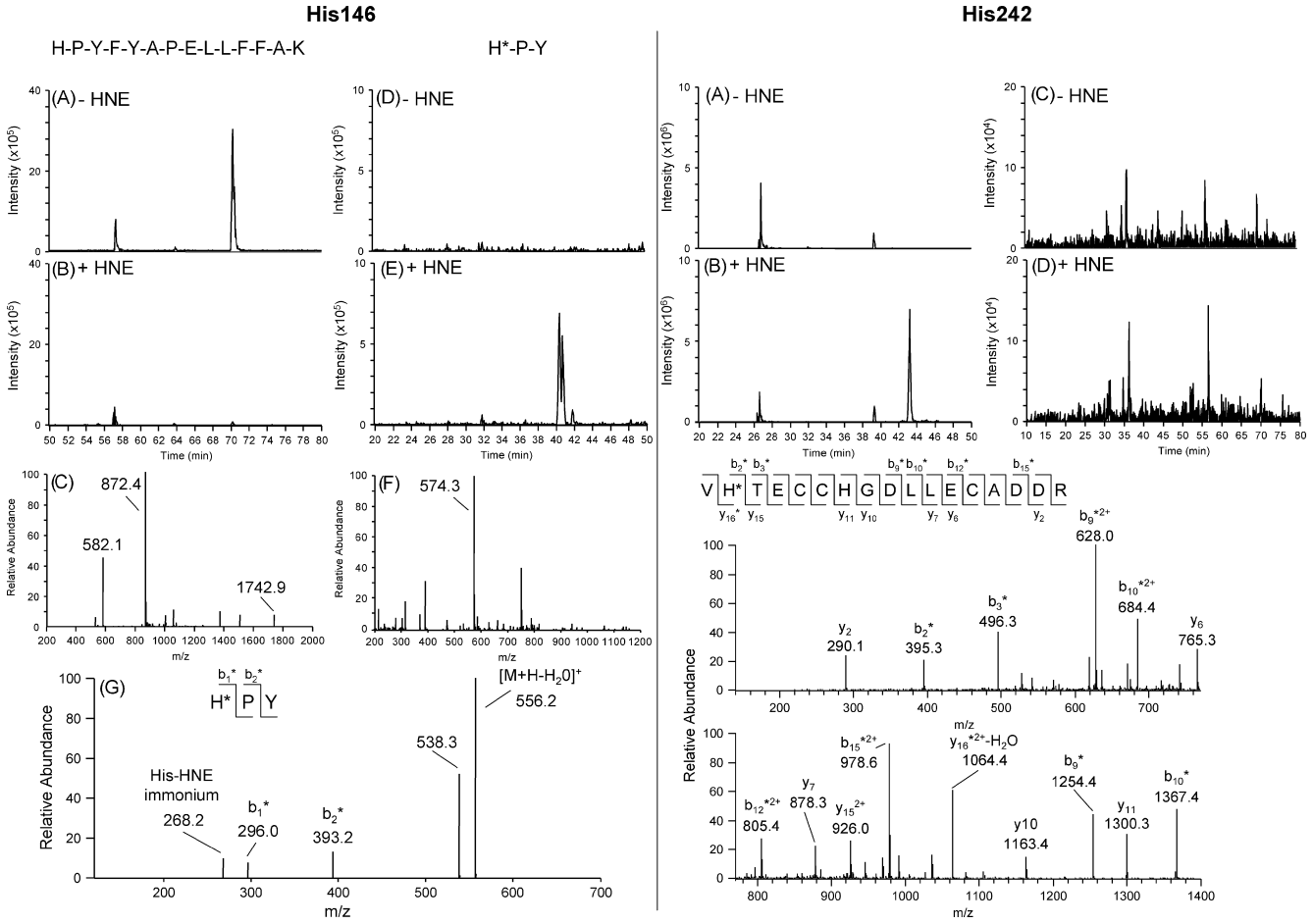

Figure 6. Identification of H-TC2 (left panel) and H-T5 (right panel) HNE-adducted peptides by LC-ESI-MS. Left side – Panels A, B: SICs relative to the ions $[M + H]^+$ m/z 1742.9 and $[M + 2H]^{2+}$ m/z 872.4 ions relative to the unmodified peptide T14. Samples are relative to HSA, incubated in the absence (panel A) and presence (panel B) of HNE (HSA : HNE 1 : 5 molar ratio) and then digested with trypsin. Panel C shows the MS spectrum relative to the peak at R.T. 70.19 min (observed mass by deconvolution analysis: 1741.9 Da; calculated mass: 1741.9 Da). Panels D, E: SICs relative to the ion $[M + H]^+$ at m/z 574.3 relative to the adducted peptide H-TC2 obtained by trypsin and chymotrypsin digestion of native (panel D) and HNE-treated HSA (panel E). Panel F shows the MS spectrum relative to the peak at R.T. 40.5 min (observed mass by deconvolution analysis: 573.3 Da; calculated mass: 573.3 Da). Panel G: LC-ESI-MS/MS spectrum of H-TC2 (parent-ion: m/z 574.3) identifying His146 as the adduction site. The symbol * denotes the shifted peptide in respect to peptides of native HSA. Right side – Panels A,B: SICs relative to the ion $[M + 2H]^{2+}$ m/z 1123.0 relative to the predicted mono HNE-adduct of peptide T25. Samples are relative to HSA incubated for 2 h at 37 °C in absence (panel A) and presence of HNE (panel B) (molar ratio HSA : HNE of 1 : 5) and then digested with trypsin. Panels C,D: SICs relative to the ion $[M + 2H]^{2+}$ m/z 1202.0 of the predicted double HNE-adducts of peptide T25; samples are relative to HSA incubated for 2 h at 37 °C in absence (panel C) and presence of HNE (panel D) (molar ratio HSA : HNE of 1 : 5) and then digested with trypsin. The LC-ESI-MS/MS spectrum of H-T5 (parent ion: m/z 749.6) permits to identify His242 as adduction site. The symbol * denotes the shifted peptide in respect to peptides form native HSA.

site of adduction was identified by MS/MS analysis of the parent-ion at m/z 749.3. His247 was excluded since the ions series remained unchanged up to y_{15} ion, while His242 was assigned as the adduction site by the presence of $y_{16}{}^{*2+} - H_2O$ at m/z 1064.4 and by the adducted $b_2{}^*$ ion at m/z 395.3 (Fig. 6, right panel).

His288

Peptide T29 is characterized by the presence of three nucleophilic sites, namely, His288, Cys289 and Lys313. However, only His288 was considered as a potential adduction site, since Cys289 is present as disulfide in the native protein; Lys313 was excluded since no consumption of peptide T30 was observed. SIC traces relative to the predicted ions confirmed this assumption, and the identification of the adducted peptide (H-T6, Table 2) was achieved by the product ion analysis of the parent ion $[M + 2H]^{2+}$, yielding an unmodified y-ion series up to the ion $y_{25}{}^{2+}$ at m/z 1375.2, the shifted $y_{26}{}^{2+}$ at m/z 1523.6, and the b-ion series (from $b_3{}^*$ to $b_{16}{}^*$) shifted of +158 Da (Fig. 7(A)).

His 510

HNE-adducted peptide T47 (HT-7, Table 2) was identified by MS/MS analysis of the parent ion $[M + 2H]^{2+}$ at m/z 1209.6, yielding a partial y ions series. The adduction site

DOI: 10.1002/jms

JMS

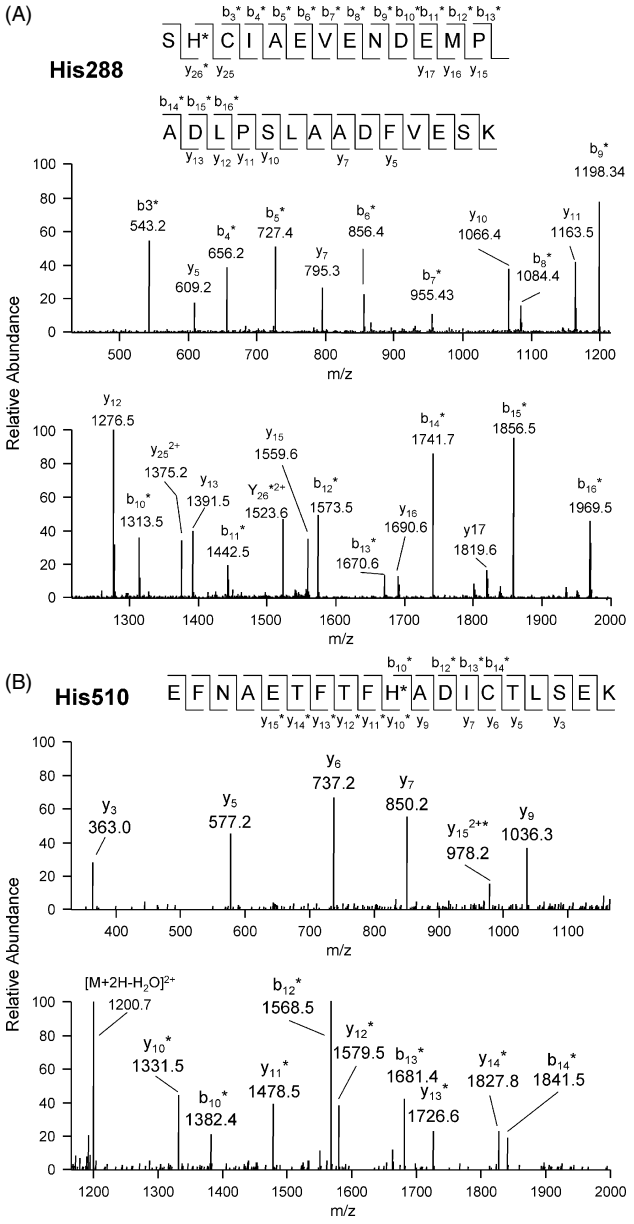

Figure 7. Identification of HNE-adduction sites of HT-6 and HT-7 by LC-ESI-MS. Upper panel: LC-ESI-MS/MS spectrum of $[M + 2H]^{2+}$ ion at m/z 1566.7 relative to H-T6. Lower panel: LC-ESI-MS/MS spectrum of $[M + 2H]^{2+}$ ion at m/z 1209.6 relative to H-T7. The symbol * denotes the shifted peptide in respect to native HSA.

was unambiguously identified by the y_9 and y_{10}^* ions at m/z 1036.3 and m/z 1331.5, respectively (Fig. 7(B)).

Cys34

Peptide T3 contains two nucleophilic sites: Cys34 and His39. In the trypsin-digested mixture, no detectable peaks were found in the reconstituted ion traces relative to the predicted adducts. Similar to His146, the adducted peptide was identified in the trypsin/chymotrypsin reaction mixture as MA of the peptide LQQCPF (H-TC1, Table 2) (Fig. 8). The adduction site was unambiguously identified by MS^2 analysis of the $[M + H]^+$ at m/z 893.3, showing unmodified b_3 ion at m/z 370.1 and a +158 shifted b_4^* ion at m/z 631.1. As an additional confirmation, the y-ion series is characterized by the native y_2 ion at m/z 263.1 and by the HNE-modified peptide y_3^* at m/z 524.2 (Fig. 8, panel D).

Reconstituted ion traces at different mass ranges: Lys195

As an additional approach for the identification/confirmation of the adducted peptides, the ion traces reconstituted at different mass ranges (m/z 300–500, 500–750, 750–1000, 1000–1500, 1500–2000) were searched for peaks absent in native HSA, but detectable in HNE-treated samples. By using this approach three peaks were identified, two of them already identified as H-T5 and H-T6, and a third unknown and characterized by a MW of 886.5 Da (Fig. 9), which corresponds to the HNE Schiff base of the merged peptide ASSAK*QR. MS^2 analysis of the $[M + H]^+$ at m/z 887.5 confirmed the identity of the peptide, and permitted to identify the adduction site as Lys195 on the basis of y_2 at m/z 303.2 and of the +158 shifted y_3^* ion at m/z 571.4 (Fig. 9, panel D).

This adducted peptide was not identified by using the quenching-peptide approach described above since both the two merged peptides, ASSAK and QR, were not mapped in the tryptic mixture.

Lys, His and Cys adducted sites: order of reactivity

Once the nucleophilic sites of albumin capable of reacting with HNE have been identified, we then evaluated which residues represent the most reactive sites and bind HNE first. To do this, the quenching-peptide method was applied to HSA samples incubated with a smaller amount of HNE with respect to HSA. In particular, when HSA was incubated with HNE at 1:0.25 molar ratio, direct infusion experiments evidenced the formation of one Michael adduct and LC-ESI-MS/MS analysis showed a significant consumption of peptide T3, owing to the HNE adduction at Cys34, as confirmed by MS^2 experiments. In addition, the SIC traces were reconstituted using as filter ions those relative to the 11 adducted peptides so far identified, and only a significant peak relative to the MA-HNE adduct (H-TC1, Table 2) was clearly detectable in the HNE-treated sample (data not shown). By increasing the molar ratio to 1:0.5 (three adducts identified in direct infusion experiments, two of them in a greater amount), the other two peptides were found to be reduced below the threshold of 10%: T14 and T18, due to His146 and Lys199 covalent adduction, respectively. Reconstituted SIC traces obtained by extracting the filter ion at m/z 574.3 confirmed the formation of H-TC2. By considering peptide T18, since HNE can react with Lys199 through both a Michael and Schiff base mechanism, the SIC traces for both the adducts were reconstituted. They showed a predominant formation of SB-HNE (H-T4) with respect to MA-HNE adduct (H-T3); these results are confirmed by direct infusion experiments which evidence the formation of a Schiff base adduct (H2), since it is characterized by a mass increase of +140 in respect to the first adduct. Hence, Cys34 appears the most reactive site of HSA toward covalent adduction of HNE, followed by Lys199, which primarily reacts through the formation of a Schiff base, and His146, giving the corresponding HNE-Michael adduct.

DOI: 10.1002/jms

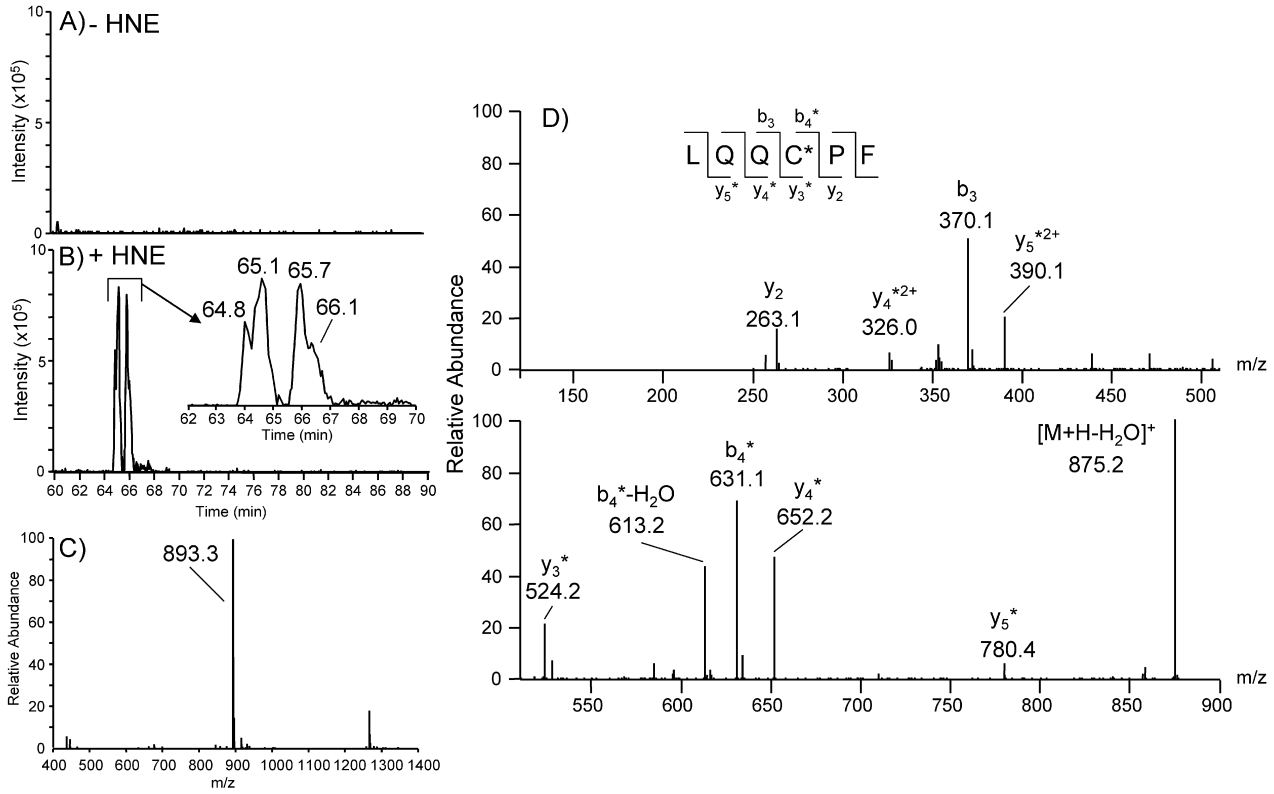

Figure 8. Identification of H-TC1 adducted peptide by LC-ESI-MS. Panels A,B: SICs relative to the HNE-Michael adduct of LQQCPF peptide $[M + H]^+$ ion at m/z 893.5; the samples are relative to trypsin-digested HSA, incubated in the absence (panel A) and presence (panel B) of HNE (HSA : HNE 1 : 5 molar ratio). Panel C shows the MS spectrum relative to the peak at R.T. 65.1 min (a super-imposable spectrum was observed for peaks relative to diasteroisomers at 64.8, 65.7 and 66.1 min, data not shown). Right panel: LC-ESI-MS/MS spectrum of H-TC1, m/z 893.3 as parent-ion. The symbol * denotes the shifted peptide in respect to peptides of native HSA.

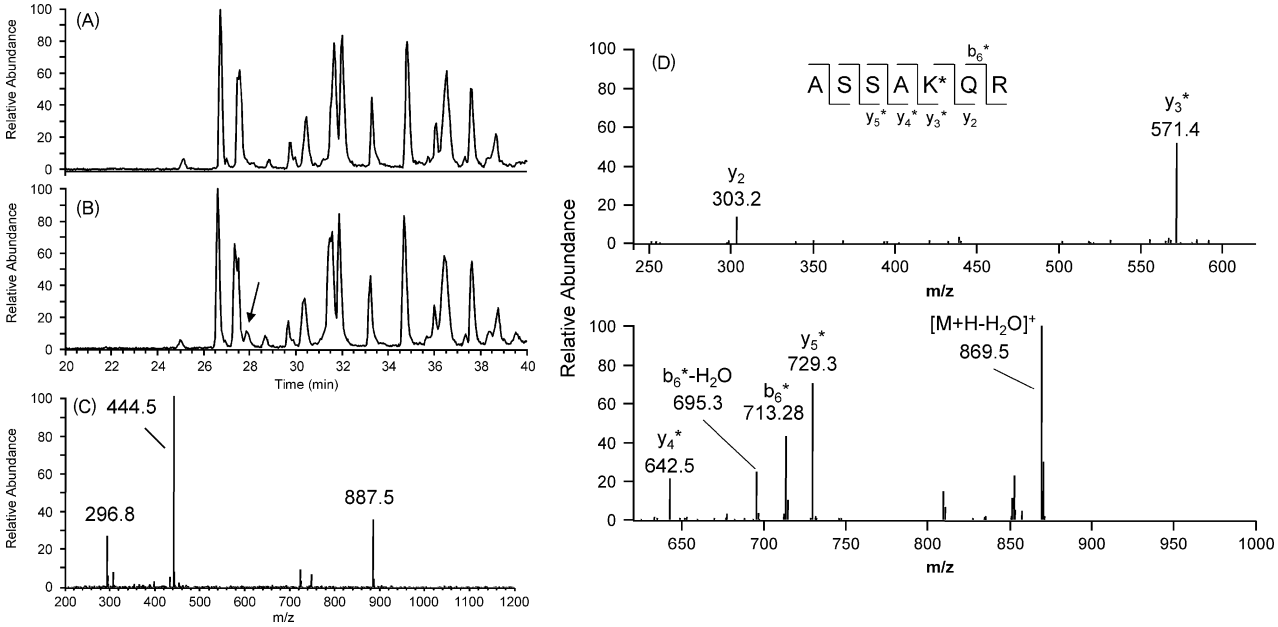

Figure 9. Identification of Lys195 as adduction site. TICs traces reconstituted using a mass range m/z 300–500 of trypsin-digested HSA; HSA was incubated in the absence (panel A) and presence (panel B) of HNE (HSA : HNE 1 : 5 molar ratio). The arrow indicates the peak at R.T. 27.8 min, which is present only in the sample of HNE-treated HSA. Panel C shows the MS spectrum relative to the peak at R.T. 27.8 min, which shows a MW of 886.5 Da, attributed to the SB of the merged peptide ASSAKQR. On the right side the LC-ESI-MS/MS spectrum setting the m/z 887.5 as parent-ion and identifying Lys195 as adduction site.

DOI: 10.1002/jms

DISCUSSION

HNE is rapidly quenched by HSA, and this is due to the covalent adduction of HNE to the different accessible nucleophilic residues of HSA. The adduction mechanism has been first demonstrated by ESI-MS direct infusion experiments, which evidenced the formation of one to nine HNE-adducts, depending on the molar ratio used. We can exclude the fact that the observed adducts are due to noncovalent binding since in the experimental conditions used, the weak associations are not preserved as they collide with the inert desolvation gas. In fact the ESI-MS spectrum of native HSA shows only three main peaks, one relative to HSA, and the other two to the covalent modified forms: the cysteinylated and glycated HSA derivatives. Noncovalent adducts of HSA with free fatty acids (HSA is known to transport fatty acids) such as HSA + palmitic acid (HSA + 258), as observed by Brennan[29] were not preserved under our conditions, and confirm that covalent adducts only are observed in the experimental conditions used.

By using a LC-ESI-MS/MS approach (quenching-peptide method), we found that HSA treated with HNE (HSA : HNE 1 : 5 molar ratio) for 2 h at 37 °C is characterized by 11 different adducts, involving 9 nucleophilic sites, as summarized in Table 2. Apparently, these results seem to be in contrast with those obtained by direct infusion experiments, in which only 9 adducts were detected. However, this discrepancy can be explained by considering the fact that both Lys199 and Lys525 were found to form both MA and SB adducts, and that MA and SB derivatives could not be distinguished by direct infusion experiments ($\Delta m = 18$ Da, $\Delta m/z = 0.38$ for +47 multicharged ion, resolution m/z 0.5).

The quenching-peptide method was then applied to HSA samples incubated with smaller amount of HNE (HSA : HNE 1 : 0.25 and 1 : 0.5), and this approach permitted the identification of the most reactive HNE-adduction sites, those that react first with HNE. The sites were identified to be Cys34 and His146, both of them giving HNE-MA adducts, and Lys199, which mainly reacts by forming the HNE-SB adduct.

Cys34 has previously been identified as a nucleophilic site capable of reacting with electrophiles such as sulphur[30] and nitrogen mustards.[31] Cys34 provides the largest fraction of free thiol in blood serum (≈80%) and mainly it accounts for the antioxidant activity of albumin, being the preferential plasma scavenger of reactive species such as hydrogen peroxide, superoxide anion, hydroxyl radical, peroxynitrite and phospholipid hydroperoxides. Freshly isolated HSA is heterogeneous with respect to its thiol content, reported as typically 0.6–0.7 SH/HSA, as confirmed in the present study. Another important and reactive binding site of HSA toward HNE is represented by His146, a nucleophilic site that has been previously reported to be the adduction site of polycyclic aromatic hydrocarbon epoxides[32] and of the butadiene metabolite epoxybutanediol.[28] Lys199 has been reported as a reactive nucleophilic site located in the IIA binding site of albumin, capable of reacting with several ligands such as benzylpenicillin, through an aminolysis reaction.[33] We found that Lys199 rapidly reacts with HNE, forming both MA and SB adducts, and this is due to its unusually low pK_A (of ≈8),[34] which implies the existence of a significant amount of the neutral form at physiological pH, and is responsible of the nucleophilic attack on the electrophilic substrates.

Owing to the growing evidences of HNE implications in several physiopathological conditions and a general consensus that HNE is a suitable biomarker of systemic oxidative stress, an analytical method capable of specifically measuring HNE in body fluids and tissues represents a stimulating challenge. Since the pioneering work of Esterbauer and his colleagues on HNE measurement in biological matrices by HPLC analysis,[35] much progress has been made, although the golden method is yet to be reached. In plasma samples, measurement of the free form of HNE has been reported by using various analytical methods, developed by applying different techniques such as HPLC,[36] GC-MS[12,37] and immunoassays.[38,39] However, HNE is highly unstable in plasma, and only a minor fraction is detected in the free form, from 2.6 nmol l^{-1} [36] to 0.65 ± 0.39 μmol l^{-1}.[37] Accordingly, Salomon[10] found that the highest levels reported of free HNE (about 0.7 nmol ml^{-1} for normal healthy individuals) accounted only about 10% of the levels of HNE-protein adducts, determined as HNE-pyrrole epitopes in the blood of healthy individuals.

Albumin modified by HNE can be a promising biomarker of circulating HNE and a systemic oxidative-stress index. In fact, aldehyde–protein adducts have a longer half-life than the corresponding free aldehydes,[40] and the relative long half-life of albumin in human subjects (15–19 days) as compared with other plasma proteins makes it an ideal biomarker of oxidative stress. In the present investigation, we found that HNE-adducted peptides and, in particular, the HNE derivatives of Cys34, His146 and Lys199 containing peptides derived by proteolytic-enzymes digestion could be suitable tags of HNE-adducted albumin. Studies are in progress to fully validate an LC-ESI-MS/MS method for the identification/quantification of these tag peptides in enzymatically digested human albumin from subjects under different physiopathological conditions.

Acknowledgements

This study was supported by COFIN2004 (Cofinanziamento Programma Nazionale 2004), Ministero dell'Università e della Ricerca.

REFERENCES

1. Esterbauer H, Schaur RJ, Zollner H. Chemistry and biochemistry of 4-hydroxynonenal, malonaldehyde and related aldehydes. *Free Radical Biol. Med.* 1991; **11**: 81.
2. Poli G, Schaur RJ. 4-Hydroxynonenal in the pathomechanisms of oxidative stress. *IUBMB Life.* 2000; **50**: 315.
3. Zarkovic N. 4-hydroxynonenal as a bioactive marker of pathophysiological processes. *Mol. Aspects Med.* 2003; **24**: 281.
4. Leonarduzzi G, Chiarpotto E, Biasi F, Poli G. 4-Hydroxynonenal and cholesterol oxidation products in atherosclerosis. *Mol. Nutr. Food Res.* 2005; **49**: 1044.
5. Carini M, Aldini G, Maffei Facino R. Sequestering agents of intermediate reactive aldehydes as inhibitors of advanced lipoxidation end-products (ALEs). In *Redox Proteomics: from Protein Modifications to Cellular Dysfunction and Diseases*, Dalle-Donne I, Scaloni A, Butterfield A (eds). Wiley InterScience Books from John Wiley & Sons: Hoboken, New Jersey, 2006; 877.

6. Sayre LM, Arora PK, Iyer RS, Salomon RG. Pyrrole formation from 4-hydroxynonenal and primary amines. *Chem. Res. Toxicol.* 1993; **6**: 19.
7. Carini M, Aldini G, Maffei Facino R. Mass spectrometry for detection of 4-hydroxy-trans-2-nonenal (HNE) adducts with peptides and proteins. *Mass Spectrom. Rev.* 2004; **23**: 281.
8. Jurgens G, Lang J, Esterbauer H. Modification of human low-density lipoprotein by the lipid peroxidation product 4-hydroxynonenal. *Biochim. Biophys. Acta* 1986; **875**: 103.
9. Bolgar MS, Yang CY, Gaskell SJ. First direct evidence for lipid/protein conjugation in oxidized human low density lipoprotein. *J. Biol. Chem.* 1996; **271**: 27999.
10. Salomon RG, Kaur K, Podrez E, Hoff HF, Krushinsky AV, Sayre LM. HNE-derived 2-pentylpyrroles are generated during oxidation of LDL, are more prevalent in blood plasma from patients with renal disease or atherosclerosis, and are present in atherosclerotic plaques. *Chem. Res. Toxicol.* 2000; **13**: 557.
11. Seidler NW, Yeargans GS. Albumin-bound polyacrolein: implications for Alzheimer's disease. *Biochem. Biophys. Res. Commun.* 2004; **320**: 213.
12. Bruenner BA, Jones AD, German JB. Simultaneous determination of multiple aldehydes in biological tissues and fluids using gas chromatography/stable isotope dilution mass spectrometry. *Anal. Biochem.* 1996; **241**: 212.
13. Toyokuni S, Yamada S, Kashima M, Ihara Y, Yamada Y, Tanaka T, Hiai H, Seino Y, Uchida K. Serum 4-hydroxy-2-nonenal-modified albumin is elevated in patients with type 2 diabetes mellitus. *Antioxid. Redox Signal.* 2000; **2**: 681.
14. Moreau R, Nguyen BT, Doneanu CE, Hagen TM. Reversal by aminoguanidine of the age-related increase in glycoxidation and lipoxidation in the cardiovascular system of Fischer 344 rats. *Biochem. Pharmacol.* 2005; **69**: 29.
15. Binder CJ, Shaw PX, Chang MK, Boullier A, Hartvigsen K, Horkko S, Miller YI, Woelkers DA, Corr M, Witztum JL. The role of natural antibodies in atherogenesis. *J. Lipid Res.* 2005; **46**: 1353.
16. Traverso N, Menini S, Cosso L, Odetti P, Albano E, Pronzato MA, Marinari UM. Immunological evidence for increased oxidative stress in diabetic rats. *Diabetologia* 1998; **41**: 265.
17. Mottaran E, Stewart SF, Rolla R, Vay D, Cipriani V, Moretti M, Vidali M, Sartori M, Rigamonti C, Day CP, Albano E. Lipid peroxidation contributes to immune reactions associated with alcoholic liver disease. *Free Radical Biol. Med.* 2002; **32**: 38.
18. Rees MS, van Kuijk FJGM, Siakotos AN, Mundy BP. Improved synthesis of various isotope labelled 4-hydroxyalkenals and peroxidation intermediates. *Synth. Commun.* 1995; **25**: 3225.
19. Aldini G, Granata P, Orioli M, Santaniello E, Carini M. Detoxification of 4-hydroxynonenal (HNE) in keratinocytes: characterization of conjugated metabolites by liquid chromatography/electrospray ionization tandem mass spectrometry. *J. Mass Spectrom.* 2003; **38**: 1160.
20. Zhang Z, Marshall AG. A universal algorithm for fast and automated charge state deconvolution of electrospray mass-to-charge ratio spectra. *J. Am. Soc. Mass Spectrom.* 1998; **9**: 225.
21. Wilkins MR, Lindskog I, Gasteiger E, Bairoch A, Sanchez JC, Hochstrasser DF, Appel RD. Detailed peptide characterisation using PEPTIDEMASS – a World-Wide Web accessible tool. *Electrophoresis* 1997; **18**: 403.
22. Feng Z, Hu W, Tang MS. Trans-4-hydroxy-2-nonenal inhibits nucleotide excision repair in human cells: a possible mechanism for lipid peroxidation-induced carcinogenesis. *Proc. Natl. Acad. Sci. U.S.A.* 2004; **101**: 8598.
23. Siems W, Grune T. Intracellular metabolism of 4-hydroxynonenal. *Mol. Aspects Med.* 2003; **24**: 167.
24. Bar-Or D, Bar-Or R, Rael LT, Gardner DK, Slone DS, Craun ML. Heterogeneity and oxidation status of commercial human albumin preparations in clinical use. *Crit. Care Med.* 2005; **33**: 1638.
25. Beck JL, Ambahera S, Yong SR, Sheil MM, de Jersey J, Ralph SF. Direct observation of covalent adducts with Cys34 of human serum albumin using mass spectrometry. *Anal. Biochem.* 2004; **325**: 326.
26. Crabb JW, O'Neil J, Miyagi M, West K, Hoff HF. Hydroxynonenal inactivates cathepsin B by forming Michael adducts with active site residues. *Protein Sci.* 2002; **11**: 831.
27. Biemann K. Contributions of mass spectrometry to peptide and protein structure. *Biomed. Environ. Mass Spectrom.* 1988; **16**: 99.
28. Lindh CH, Kristiansson MH, Berg-Andersson UA, Cohen AS. Characterization of adducts formed between human serum albumin and the butadiene metabolite epoxybutanediol. *Rapid Commun. Mass Spectrom.* 2005; **19**: 2488.
29. Brennan SO. Electrospray ionization mass analysis of normal and genetic variants of human serum albumin. *Clin. Chem.* 1998; **44**: 2264.
30. Noort D, Hulst AG, de Jong LP, Benschop HP. Alkylation of human serum albumin by sulfur mustard in vitro and in vivo: mass spectrometric analysis of a cysteine adduct as a sensitive biomarker of exposure. *Chem. Res. Toxicol.* 1999; **12**: 715.
31. Noort D, Hulst AG, Jansen R. Covalent binding of nitrogen mustards to the cysteine-34 residue in human serum albumin. *Arch. Toxicol.* 2002; **76**: 83.
32. Brunmark P, Harriman S, Skipper PL, Wishnok JS, Amin S, Tannenbaum SR. Identification of subdomain IB in human serum albumin as a major binding site for polycyclic aromatic hydrocarbon epoxides. *Chem. Res. Toxicol.* 1997; **10**: 880.
33. Diaz N, Suarez D, Sordo TL, Merz KM Jr. A theoretical study of the aminolysis reaction of lysine 199 of human serum albumin with benzylpenicillin: consequences for immunochemistry of penicillins. *J. Am. Chem. Soc.* 2001; **123**: 7574.
34. Diaz N, Suarez D, Sordo TL, Merz KM Jr. Molecular dynamics study of the IIA binding site in human serum albumin: influence of the protonation state of Lys195 and Lys199. *J. Med. Chem.* 2001; **44**: 250.
35. Esterbauer H, Cheeseman KH. Determination of aldehydic lipid peroxidation products: malonaldehyde and 4-hydroxynonenal. *Methods Enzymol.* 1990; **186**: 407.
36. Strohmaier H, Hinghofer-Szalkay H, Schaur RJ. Detection of 4-hydroxynonenal (HNE) as a physiological component in human plasma. *J. Lipid Mediat. Cell Signal.* 1995; **11**: 51.
37. Spies-Martin D, Sommerburg O, Langhans CD, Leichsenring M. Measurement of 4-hydroxynonenal in small volume blood plasma samples: modification of a gas chromatographic-mass spectrometric method for clinical settings. *J. Chromatogr. B Analyt. Technol. Biomed. Life Sci.* 2002; **774**: 231.
38. Uchida K, Osawa T, Hiai H, Toyokuni S. 4-Hydroxy-2-nonenal-trapping ELISA: direct evidence for the release of a cytotoxic aldehyde from oxidized low density lipoproteins. *Biochem. Biophys. Res. Commun.* 1995; **212**: 1068.
39. Kimura H, Liu S, Yamada S, Uchida K, Matsumoto K, Mukaida M, Yoshida K. Rapid increase in serum lipid peroxide 4-hydroxynonenal (HNE) through monocyte NADPH oxidase in early endo-toxemia. *Free Radic. Res.* 2005; **39**: 845.
40. Bruenner BA, Jones AD, German JB. Direct characterization of protein adducts of the lipid peroxidation product 4-hydroxy-2-nonenal using electrospray mass spectrometry. *Chem. Res. Toxicol.* 1995; **8**: 552.